Talanta 115 (2013) 801–805

Contents lists available at SciVerse ScienceDirect

Talanta

journal homepage: www.elsevier.com/locate/talanta

A novel organic–inorganic hybrid monolithic column prepared in-situ in a microchip and its application for the determination of 2-amino-4-chlorophenol in chlorzoxazone tablets

Junling Zhang [a], Gang Chen [a], Miaomiao Tian [a], Ruigang Li [b], Xinjun Quan [a], Qiong Jia [a,*]

[a] College of Chemistry, Jilin University, Qianjin Street 2699#, Changchun, 130012, PR China
[b] Key Laboratory of Optical System Advanced Manufacturing Technology, Changchun Institute of Optics, Fine Mechanics and Physics, Chinese Academy of Sciences, Changchun 130033, China

ARTICLE INFO

Article history:
Received 19 April 2013
Received in revised form
21 June 2013
Accepted 28 June 2013
Available online 4 July 2013

Keywords:
Organic–inorganic hybrid monolith
Microfluidic chip
2-amino-4-chlorophenol
Solid phase microextraction
Optical fiber spectrophotometry

ABSTRACT

γ-Alumina nanoparticles (γ-Al_2O_3) were introduced to the conventional poly(methacrylic acid-*co*-ethylene glycol dimethacrylate) (MAA-*co*-EGDMA) monolith to prepare a novel organic-inorganic hybrid monolith, poly(MAA-*co*-EGDMA)-Al_2O_3 monolith. The polymerization was induced in-situ with UV irradiation in an ultraviolet transparent polymethyl methacrylate (PMMA) microfluidic chip. The monolith-based solid phase microextraction system was used for the on-line determination of 2-amino-4-chlorophenol (ACP) in chlorzoxazone tablets coupled with an optical fiber spectrophotometer. Several parameters affecting the adsorption/desorption, including sample pH value, sample flow rate, sampling time, eluent flow rate, and eluting time, were investigated in detail. Under the optimized conditions, limit of detection (LOD) and limit of quantification (LOQ) of the method were calculated to be 2.8 and 9.1 μg L^{-1}, respectively, with the relative standard deviation (RSD) of 3.1%.

1. Introduction

Interests in microfabricated devices designed for micro total analytical systems (μ-TAS) which integrates sample delivery, separation, and detection on miniaturized devices continue to grow almost unabated since it was first proposed by Manz et al. [1]. As a result of miniaturization, sophisticated setup, and possible multiplexing, analytical microchip has exerted great potential in many fields such as clinical laboratory science, pharmaceutical synthesis and screening, research on relationship between human genetics and diseases, food and commodity inspection, environment monitoring, criminal science, military science, space science, and so on [2]. In recent years, it has been gradually extended to many sides of chemical and biological analysis. In particular, sample pretreatment procedures such as concentration enhancement can be one of the major focuses of microchip especially when analyzing very dilute samples [3–5].

Sample preconcentration is necessary prior to analysis in instances where trace analysis is desired and the detection sensitivity is too low to reliably detect and quantify analytes. Various sample pretreatment systems based on microfludic chip, including liquid–liquid extraction (LLE) [6], liquid-liquid membrane extraction (LLME), solid-phase extraction (SPE) [4], and solid phase microextraction (SPME) [7–10], have been studied. SPME is a well-characterized technique introduced by Pawliszyn and co-workers in the early 1990s [11,12]. It is a solvent-free extraction method which not only reduces solvent and sample consumption, but also lowers the method detection limit [7]. SPME has been successfully adapted to microdevices to accomplish reduced-volume and high-efficiency extractions for catechins [7], dopamine [8], heavy metals [9], proteomic sample [10], and so on.

Extraction materials for SPME currently include magnetic materials [9,13], membranes [14,15], and polymer monolithic columns [7,16], etc. Polymer monolithic column is one kind of promising sorbent materials because it can be easily synthesized in situ and provides tunable monolithic structures with tailored functional groups for specific purposes. Moreover, the monolithic porous structure offers convective mass transfer procedure, which is preferable in extraction processes. However, the relatively low surface area is one of the limitations of polymer monoliths to be used as adsorption materials according to Potter's critical review [17]. Moreover, the swelling behavior of polymer monoliths in organic solvents is another limitation which will cause changes of pore structure and poor mechanical stability. In order to solve these problems, a new approach to functionalize polymer monoliths with nanomaterials has been developed. Considering the large surface-to-volume ratio, excellent mechanical properties and multiform morphologies which potentially facilitates mass transfer, inorganic

* Corresponding author. Tel.: +86-431-85095621.
E-mail address: jiaqiong@jlu.edu.cn (Q. Jia).

0039-9140/$ - see front matter © 2013 Elsevier B.V. All rights reserved.
http://dx.doi.org/10.1016/j.talanta.2013.06.058

nanoparticles are outstanding functionalization materials. In Krenkova's study [18], rod-shaped hydroxyapatite nanoparticles were incorporated into the poly(2-hydroxyethyl methacrylate-*co*-ethylene dimethacrylate) monolith. The monolith can provide a high speed at which these columns can be used to selectively enrich and separate phosphopeptides from complex peptide mixtures of ovalbumin, γ-casein, and β-casein digests. Afterwards, Krenkova and co-workers [19] developed a new type of iron oxide nanoparticle coating for organic polymer monolith for phosphopeptide enrichment from peptide mixtures. Thabano et al. [20] prepared silica nanoparticle-templated methacrylic acid monoliths for in-line preconcentration and separation of neurotransmitters. Injection time allowed by this monolith was increased 10 times over that of an untemplated monolith which provides increased adsorption capacity predominantly.

γ-Alumina (Al_2O_3) has not only common characteristics of inorganic nanoparticles such as large surface area, high porosity, strong ability of adsorption, but also excellent dispersibility in many organic solvents. In our previous work [21], poly(*N*-isopropylacrylamide-*co*-*N*, *N*'-methylene bisacrylamide) monolithic column embedded with γ-alumina nanoparticles was prepared and applied to the extraction of synthetic food dyes in soft drink samples with satisfactory results. It can be expected that γ-alumina may be easily incorporated into poly(methacrylic acid-*co*-ethylene glycol dimethacrylate) (MAA-*co*-EGDMA) monolith by homogeneously dispersed in porogens to develop a hybrid poly (MAA-*co*-EGDMA)-Al_2O_3 monolith.

2-amino-4-chlorophenol (ACP) is used as an important intermediate in the chemical and pharmaceutical industries, and as a raw material in dye manufacture [22]. However, ACP is reported to possess a stimulative property that causes irritation and contact dermatitis. As one kind of medicine employing ACP as intermediate, chlorzoxazone tablet is an effective muscle relaxant in the treatment of painful muscle spasm [23]. Considering of its harms to peoples' health, the determination of the residual ACP in chlorzoxazone tablets is necessary. In this work, we synthesized the poly(MAA-*co*-EGDMA)-Al_2O_3 monolith in a microfluidic chip induced with UV irradiation. The monolith was combined with an optical fiber spectrophotometer to determine ACP in chlorzoxazone tablets.

2. Experimental

2.1. Materials and instrumentation

Methacrylic acid (MAA), *n*-hexane, HPLC grade methanol, and azobisisobutyronitrile (AIBN) were purchased from Tianjin Chemical Plant (Tianjin, China). Ethylene glycol dimethacrylate (EGDMA) was provided by TCI (Tokyo, Japan). 3-(Trimethoxysilyl) propyl methacrylate and γ-Al_2O_3 (10 nm) were obtained from Aladdin Reagent (Shanghai, China). Chlorzoxazone tablets were purchased from medicamentarius in Changchun. A stock solution of ACP (1000 mg L^{-1}) was prepared by dissolving 0.1 g ACP (Aladdin Reagent, Shanghai) with 0.02 mol L^{-1} HNO_3 and made up to 100 mL by double distilled water. MAA and EGDMA were filtrated with 0.45 μm filtering membrane before use. AIBN was purified by recrystallization from ethanol and then dried in vacuum drying oven at room temperature.

An LSP01-1 A programmable syringe pump (Baoding Longer Precision Pump Co., Ltd., Hebei, China) was used for pushing solutions. For pH measurements, a pH-3C digital pH meter (Shanghai Rex Instruments Factory, China) was employed. Fourier-transformed infrared spectra (FTIR) was obtained using Thermo Nicolet 670 FTIR instrument (Thermo, USA). The microscopic morphology was observed by S4800 ESEM Hitachi microscope (SEM, Hitachi, Japan). Double distilled water used for all the experiments was prepared by the Milli-Q SP system (Millipore, Milford, MA, USA). ZF-1 triplepurpose ultraviolet analyzer (Jinpeng analysis instrument Co., Ltd., Shanghai, China) was used for photoinitiating the polymerization reaction. Spectrophotometric measurements were carried out at 230 nm using a refit Ocean optics UV–vis spectrometer (USB 4000, Ocean Optics Inc., Dunedin, USA) with a UV light (Analytical Instrument Systems, Inc., Flemington, USA). Two fiber-optic cables furnished with a stainless steel clad tip (400 μm i.d.) were used to connect the flow cell to the light source of the spectrometer.

2.2. Microfluidic chip

2.2.1. Preparation of microfluidic chip

A simple straight microchannel (300 μm wide, 300 μm deep, 5 cm long) containing a separation part (500 μm wide, 500 μm deep, 2 cm long) was fabricated on a poly(methyl methacrylate)

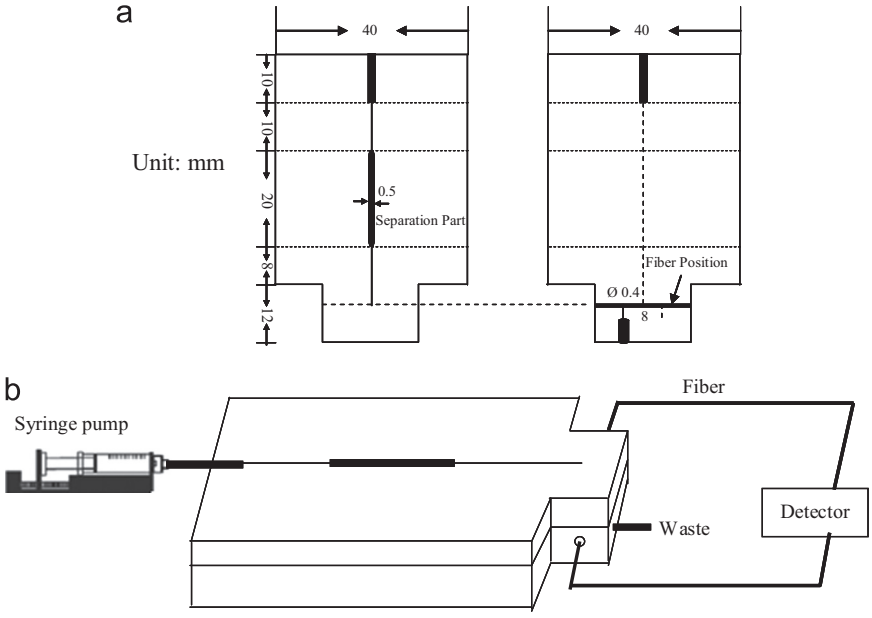

Fig. 1. Dimension diagrams of the microfluid chips (a) and assembly drawing of microchip and Ocean Optics UV–vis spectrometer (b).

(PMMA) plate. A channel (φ=400 μm, 20 mm long) for a refit fiber spectrophotometer was fabricated in the other PMMA plate. The end point of the straight microchannel and the channel for the optical fiber-type spectrophotometer was connected with another vertical channel. The two PMMA plates were then adhered in a constant-temperature oven with the temperature rising 5 °C each half an hour from 100 °C to 120 °C. Fig. 1 showed the dimension diagram of the microfluidic chip, the assembly drawing of microchip, and Ocean Optics UV–vis spectrometer.

2.2.2. Photopolymerization of hybrid monolith in microfluidic chip

The microchannel was activated before use and the definite procedure was as follows. Firstly, the microchannel was rinsed with ethanol and double distilled water using a syringe, activated with 0.2 mol L^{-1} sodium hydroxide for 30 min, washed with water followed by 0.2 mol L^{-1} HCl for 30 min, washed with double distilled water and ethanol successively, and dried at 100 °C for 1 h. Finally, the microchannel was filled with a 3-(trimethoxysilyl)propyl methacrylate (30% in ethanol, V/V), sealed, and left to react for 24 h at room temperature to enable covalent attachment of the monolith. The vinylized channel was washed with ethanol and dried with N_2.

25 mg γ-Al_2O_3 was dispersed uniformly in the porogens, 805 mg methanol, and 290 mg *n*-hexane. The dispersion was then mixed with 48 mg monomer (MAA), 420 mg crosslinker (EGDMA), and 4.5 mg initiator (AIBN). The mixture was sonicated to achieve a homogeneous solution and then purged with N_2 for 10 min to remove O_2. The mixture was pumped into the microchannel and the microchip was then sealed with the tape. The surface of the chip was covered with tinfoil just leaving the separation part to be exposed to the UV light. The polymerization reaction was allowed to proceed for 3 h under the UV light of 365 nm. After the reaction finished, the monolith was washed with ethanol to remove the unreacted components.

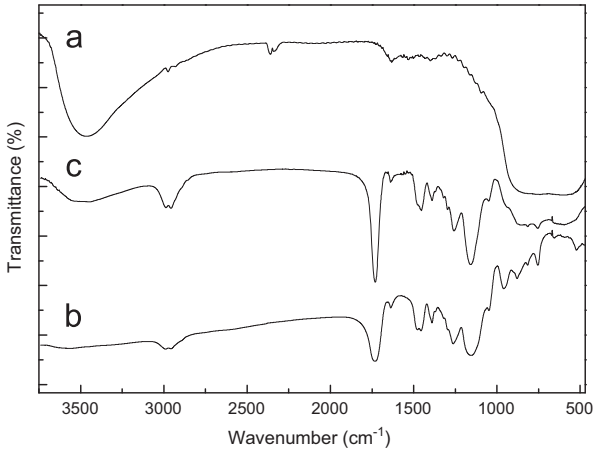

Fig. 2. FT-IR spectra of γ-Al_2O_3 (a), poly(MAA-*co*-EGDMA) (b), and poly(MAA-*co*-EGDMA)- γ-Al_2O_3 (c).

2.3. Procedure of solid phase microextraction

The typical procedure of on-line solid phase microextraction and determination of ACP was as follows. At the beginning, the syringe was filled with 0.3 mL methanol and pushed through the microchannel at the flow rate of 50 μL min^{-1}, followed by 0.5 mL phosphate buffer (pH 5.0) for monolith preconditioning. Then the sample (pH 5.0) was drawn through the microchannel at the speed of 70 μL min^{-1} for 235 s. Then 0.3 mL phosphate buffer solution was injected to remove the residual matrix and the residual solution was driven out by air via a clean syringe. In the elution step, methanol was propelled through the microchannel at a flow rate of 50 μL min^{-1} for 170 s to elute the ACP retained on the monolith and the eluent solution was determined by the spectrometer immediately. All the experimental work was carried out in triplicate and the average result was presented.

2.4. Sample preparation

ACP solutions with different concentrations were prepared by diluting the 1000 μg mL^{-1} stock solution. Chlorzoxazone tablets were pulverized and 0.3000 g powder was dissolved by dilute nitric acid, filtered by 0.45 μm filter membrane and diluted to 100 mL by double distilled water. During the process, we prepared every sample in double. One was handled according to the procedure mentioned above, and the other was spiked with 50 μg g^{-1} standard solution for the recovery tests.

3. Results and discussion

3.1. Characterizations of the monolith materials

FT-IR with 16 scan times was employed to characterize γ-Al_2O_3, poly(MAA-*co*-EGDMA), and poly(MAA-*co*-EGDMA)-γ-Al_2O_3 monolith, where poly(MAA-*co*-EGDMA) was prepared similar to poly (MAA-*co*-EGDMA)-γ-Al_2O_3 (Section 2.2.2) but without the step of adding γ-Al_2O_3. Results were shown in Fig. 2. In Fig. 2(a), the peak in wave number ranged from 400 cm^{-1} to 1000 cm^{-1} represents the characteristic infrared absorption spectrum, which is in agreement with previous literatures [24]. The peak around 3500 cm^{-1} is the stretching vibration peak of adsorbed water [25] and some residual

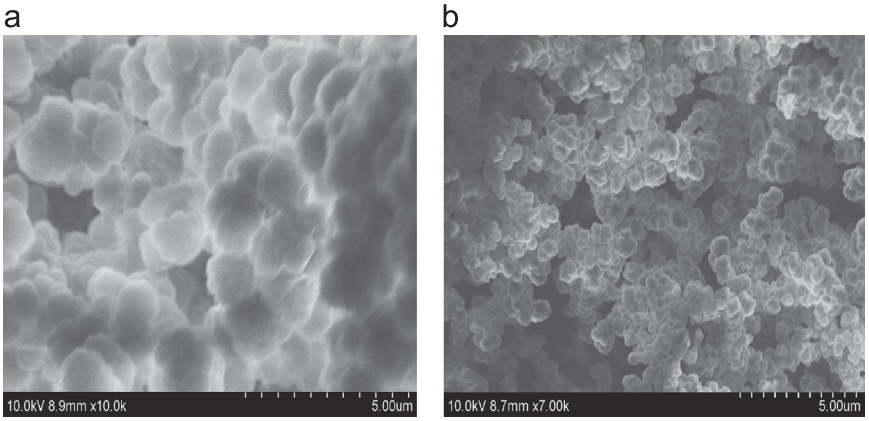

Fig. 3. SEM micrographs of poly(MAA-*co*-EGDMA) monolith (a) and poly(MAA-*co*-EGDMA)-γ-Al_2O_3 monolith (b).

hydroxyl groups. It is obvious that these peaks also appear in Fig. 2 (c), i.e., the FT-IR spectrum of poly(MAA-*co*-EGDMA)-γ-Al_2O_3. Meantime, both Figs. 2(b) and 2(c) showed the symmetric stretching vibration peak (1160 cm^{-1}), asymmetric stretching vibration peak (1050 cm^{-1}) of C−O−C, stretching vibration peak of C=C (1680 cm^{-1}), stretching vibration peak of C=O (1720 cm^{-1}), stretching vibration peak (2960 cm^{-1}), and in-plane flexural vibration peak (1460 cm^{-1}) of $-CH_3$. In conclusion, the hybrid monolith is a combination of poly(MAA-*co*-EGDMA) and γ-Al_2O_3.

The morphology of poly(MAA-*co*-EGDMA) monolith and poly (MAA-*co*-EGDMA)-γ-Al_2O_3 monolith was investigated by SEM analysis. Results were presented in Fig. 3. The micrographs demonstrated that the size of the microglobules in poly(MAA-*co*-EGDMA)-γ-Al_2O_3 monolith was smaller than those in poly (MAA-*co*-EGDMA) monolith. This could be because that excellent mechanical property of γ-Al_2O_3 improved the degree of aggregation of monolith. In addition, it could be clearly seen that the specific surface area increased after the modification.

3.2. Optimization of experimental conditions

Several experimental parameters affecting the adsorption/desorption, including sample pH value, sample flow rate, sampling time, eluent flow rate, and eluting time, were investigated to obtain the best detection conditions.

Sample pH value which influences the molecule form of the analyte, relates closely to the interactions between the analyte and the extraction phase. Considering that the solution became cloudy at pH≥8, the pH of the sample solution was optimized in the range of 1.0–7.0. As could be seen from Fig. 4(a), the absorbance was highest at pH 5.0. This may be explained as follows. In the extraction process, both hydrophobic interaction and ion-exchange resulting from the polymer backbone and its acidic pendant groups existed [26,27]. Under the acidic condition, ACP exists in the protonated form and can be extracted by ion-exchange interaction with the ionized carboxylic groups. However, the amount of ionized carboxylic groups decreases with the decrease of the matrix pH, resulting in the weakening of ion-exchange interaction. So the absorbance is growing higher when pH value is from 1.0 to 5.0. When pH is over 5.0, the absorbance decreases because ACP tends to be in its neutral or near-neutral conditions, resulting in the decrease of the ion-exchange interaction. Accordingly, pH 5.0 was selected for the subsequent analysis.

Sample flow rate directly affects adsorption efficiency. Appropriate sample flow rate should not only ensure adequate sample volumes but also ensure the thoroughly contact between the sample and the sorbent material to reach high adsorption efficiency. The sample flow rate ranging from 30 μL min^{-1} to 90 μL min^{-1} was investigated. As shown in Fig. 4(b), the absorbance increased with increasing sample flow rates. However, when the sample flow rate was over 70 μL min^{-1}, the absorbance increased slightly. Therefore, 70 μL min^{-1} was used in next steps.

A sampling timing diagram can be used to indicate the monolith's adsorption saturation point for ACP clearly. Results showed that the absorbance began to flatten when sampling time was over 235 s, which stated 235 s was the time of adsorption saturation point. Therefore, 235 s was chosen to be the optimized sampling time.

The eluent flow rate influences absorbance by affecting elution efficiency. Flow rates of methanol in the range of 30−80 μL min^{-1} were studied when other experimental conditions were fixed. Results were shown in Fig. 4(c), from which it could be concluded that the absorbance reached maximum when the flow rate of methanol was 50 μL min^{-1}. When the flow rate exceeded 50 μL min^{-1}, the absorbance decreased because high flow rate decreased contact time of ACP and methanol which was unfavorable for the release of ACP from the surface of the monolith. Therefore, 50 μL min^{-1} was used for further experiments.

When elution flow rate was fixed, eluting time was equivalent to eluent volume, the value of which was directly related to enrichment factor (EF). Results were shown in Fig. 4(d), indicating that the absorbance was growing higher until the eluting time was 170 s and then the absorbance value decreased gradually. This could be attributed to that the excess methanol diluted the analyte

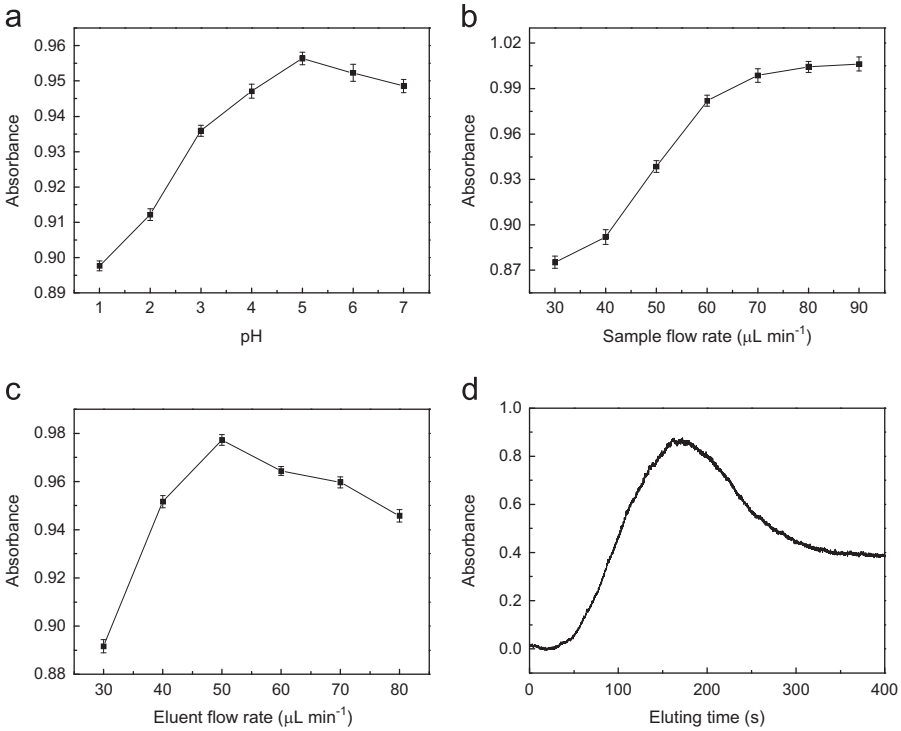

Fig. 4. Optimization experiments.

Table 1
Determination of ACP in chlorzoxazone tablets by the developed method ($n=3$).

	Found ($\mu g\ g^{-1}$)	Added ($\mu g\ g^{-1}$)	Recovery (%)
Sample 1	< LOD	50	103.4 ± 4.6
Sample 2	3.6 ± 0.1	50	93.2 ± 3.1
Sample 3	4.1 ± 0.2	50	95.7 ± 2.4

to some extent. As a result, 170 s was selected for the experiment in order to achieve the best detection effects.

3.3. Performance and applications of the method

Under the above optimized conditions, the method was validated. Within the concentration range of 2–200 $\mu g\ mL^{-1}$, the calibration curve was obtained as $A=0.3410C\ -1.5400$ ($R^2=0.9974$). Other performances of the SPME method in the microchip were also investigated. Limits of detection (LOD) and limits of quantification (LOQ) calculated with the *S*/*N* set at 3 and 10 were 2.8 and 9.1 $\mu g\ L^{-1}$, respectively. The relative standard deviation (RSD) for 7 times detections was 3.1%. The EF value obtained by the ratio of the slopes of calibration curves with/without employing the SPME method was calculated as 17.0. In order to further illustrate whether the addition of γ-Al_2O_3 benefit the extraction performance or not, the EF value was also determined with the slopes of calibration curves obtained with the poly(MAA-*co*-EGDMA) monolith and that without the SPME step. EF was calculated as 7.3, demonstrating that poly(MAA-*co*-EGDMA)-γ-Al_2O_3 monolith had higher extraction abilities compared with poly (MAA-*co*-EGDMA) monolith.

In addition, the stability of the method was investigated. Results showed that no significant variation of the extraction efficiency was verified after two months of operation. The PMMA plates, microchannels, and connections did not deteriorate during the experiments, either. The stabilities of the monolithic material and microchip provided the suitability and feasibility of the preconcentration performance of the present method.

The method was used to determine ACP in chlorzoxazone tablets produced from different pharmaceutical factories. Results were listed in Table 1, demonstrating that the recoveries with standard addition were in the range of 93.2–103.4%.

4. Conclusions

In this paper, we in-situ synthetized a hybrid monolith in a microfluidic chip as a novel adsorption material of solid phase microextraction to provide a convenient and robust method for the on-line determination of ACP. The method had many practical advantages, such as its simple and fast pretreatment procedure, low sample consumption, environment friendly, ease of use and good precision. Therefore, the proposed method provided a useful and practical approach that could be applied to detect more analytes in real samples.

Acknowledgments

The project was supported by the National Natural Science Foundation of China (21205047), the Jilin Provincial Science & Technology Department (201105102), and the Open Project of State Key Laboratory of Supramolecular Structure and Materials, Jilin University (sklssm201218).

References

[1] A. Manz, N. Graber, H.M. Widmer, Sensors Actuators B: Chem. 1 (1990) 244–248.
[2] Z.L. Fang, Q. Fang, Modern Sci. Instrum. 4 (2001) 3–6.
[3] B.S. Broyles, S.C. Jacobson, J.M. Ramsey, Anal. Chem. 75 (2003) 2761–2767.
[4] L.A. Legendre, J.M. Bienvenue, M.G. Roper, J.P. Ferrance, J.P. Landers, Anal. Chem. 78 (2006) 1444–1451.
[5] R.D. Oleschuk, L.L. Shultz-Lockyear, Y.B. Ning, D.J. Harrison, Anal. Chem. 72 (2000) 585–590.
[6] H. Shen, Q. Fang, Talanta 77 (2008) 269–272.
[7] L. Lin, H. Chen, H. Wei, F. Wang, J.-M. Lin, Analyst 136 (2011) 4260–4267.
[8] Q.S. Kang, Y. Li, J.Q. Xu, L.J. Su, Y.T. Li, W.H. Huang, Electrophoresis 31 (2010) 3028–3034.
[9] B. Chen, S. Heng, H. Peng, B. Hu, X. Yu, Z. Zhang, D. Pang, X. Yue, Y. Zhu, J. Anal. At. Spectrom. 25 (2010) 1931–1938.
[10] J. Bergkvist, S. Ekstrom, L. Wallman, M. Lofgren, G. Marko-Varga, J. Nilsson, T. Laurell, Proteomics 2 (2002) 422–429.
[11] C.L. Arthur, J. Pawliszyn, Anal. Chem. 62 (1990) 2145–2148.
[12] C.L. Arthur, L.M. Killam, K.D. Buchholz, J. Pawliszyn, J.R. Berg, Anal. Chem. 64 (1992) 1960–1966.
[13] J. Meng, J. Bu, C. Deng, X. Zhang, J. Chromatogr. A 1218 (2011) 1585–1591.
[14] C. Wu, Y. Liu, Q. Wu, C. Wang, Z. Wang, Food Anal. Methods 5 (2012) 540–550.
[15] Y. Hu, Y. Yang, J. Huang, G. Li, Anal. Chim. Acta 543 (2005) 17–24.
[16] Y. Wen, B.S. Zhou, Y. Xu, S.W. Jin, Y.Q. Feng, J. Chromatogr. A 1133 (2006) 21–28.
[17] O.G. Potter, E.F. Hilder, J. Sep. Sci. 31 (2008) 1881–1906.
[18] J. Krenkova, N.A. Lacher, F. Svec, Anal. Chem. 82 (2010) 8335–8341.
[19] J. Krenkova, F. Foret, J. Sep. Sci. 34 (2011) 2106–2112.
[20] J.R.E. Thabano, M.C. Breadmore, J.P. Hutchinson, C. Johns, P.R. Haddad, J. Chromatogr. A 1216 (2009) 4933–4940.
[21] W.J. Li, X. Zhou, S.S. Tong, Q. Jia, Talanta 105 (2013) 386–392.
[22] K. Yamazaki, M. Suzuki, H. Kano, Y. Umeda, M. Matsumoto, M. Asakura, K. Nagano, H. Arito, S. Fukushima, J. Occup. Health 51 (2009) 249–260.
[23] J.C. Abbar, S.T. Nandibewoor, Ind. Eng. Chem. Res. 51 (2012) 111–118.
[24] C.H. Shek, J.K.L. Lai, T.S. Gu, G.M. Lin, Nanostruct. Mater. 8 (1997) 605–610.
[25] C. Zhang, F. Zhap, J. Zhang, X. Wang, C. Bao, Acta Chim. Sinica 57 (1999) 275–280.
[26] T. Li, Z.G. Shi, M.M. Zheng, Y.Q. Feng, J. Chromatogr. A 1205 (2008) 163–170.
[27] F. Wei, J. Fan, M.M. Zheng, Y.Q. Feng, Electrophoresis 31 (2010) 714–723.